Inorganic Chemistry

pubs.acs.org/IC

Article

Crystalline Hydrogen-Bonding Networks and Mixed-Metal Framework Materials Enabled by an Electronically Differentiated Heteroditopic Isocyanide/Carboxylate Linker Group

Krista P. Balto, Milan Gembicky, Arnold L. Rheingold, and Joshua S. Figueroa*

Cite This: *Inorg. Chem.* 2021, 60, 12545−12554

Read Online

ACCESS | Metrics & More | Article Recommendations | Supporting Information

ABSTRACT: Mixed-metal solid-state framework materials are emerging candidates for advanced applications in catalysis and chemical separations. Traditionally, the syntheses of mixed-metal framework systems rely on postsynthetic ion exchange, metalloligands, or metal-deposition techniques for the incorporation of a second metal within a framework material. However, these methods are often incompatible with the incorporation of low-valent metal centers, which preferentially bind to electronically "soft" ligands according to the tenets of hard/soft acid/base theory. Here we present the electronically differentiated isocyanide/carboxylate heteroditopic linker ligand 1,4-CNAr^{Mes2}C$_6$H$_4$CO$_2$H (TIB^{Mes2}H; TIB = terphenyl isocyanide benzoate; Ar^{Mes2} = 2,6-(2,4,6-Me$_3$C$_6$H$_2$)$_2$C$_6$H$_2$), which is capable of selective binding of low-valent metals via the isocyano group and complexation of hard Lewis acidic metals through the carboxylate unit. This heteroditopic ligand also possesses an encumbering *m*-terphenyl backbone at the isocyanide function to foster coordinative unsaturation. The treatment of TIB^{Mes2}H with [Cu(NCMe)$_4$]PF$_6$ in a 3:1 ratio results in preferential binding of the isocyanide group to the Cu(I) center as assayed by multinuclear NMR and IR spectroscopies. IR spectroscopy also provides strong evidence for the formation of a copper(I) tris(isocyanide) complex, wherein the carboxylic acid group remains unperturbed. The addition of TIB^{Mes2} to [Cu(NCMe)$_4$]PF$_6$ in a 4:1 ratio results in crystallization of the hydrogen-bonding network, [Cu(TIB^{Mes2}H)$_4$]PF$_6$, in which the formation of $R_2^2(8)$ hydrogen bonds results in a 7-fold interpenetrated diamondoid lattice structure. The preassembly of a copper(I) tris(isocyanide) complex using TIB^{Mes2}H, followed by deprotonation and the introduction of ZnCl$_2$, generates a novel and unusual zwitterionic solid-state phase (denoted as Cu/Zn-^{ISO}CN-5; ^{ISO}CN = isocyanide coordination network) consisting of a coordinatively unsaturated [Cu(CNR)$_3$]$^+$ cationic secondary building unit (SBU) and an anionic, paddlewheel-type Zn(II)-based SBU of the formulation [Cl$_2$Zn$_2$(O$_2$CR)$_3$]$^-$. Inductively coupled plasma mass spectrometry analysis provided firm evidence for a 2:1 Zn-to-Cu ratio in the network, thereby indicating that the isocyanide and carboxylate groups selectively bind soft and hard Lewis acidic metal centers, respectively. The extended structure of Cu/Zn-^{ISO}CN-5 is a densely packed, noninterpenetrated AB-stacked layer network with modest surface area. However, it is thermally robust, and its formation and compositional integrity validate the use of an electronically differentiated linker for the formation of mixed-metal frameworks incorporating low-valent metal centers.

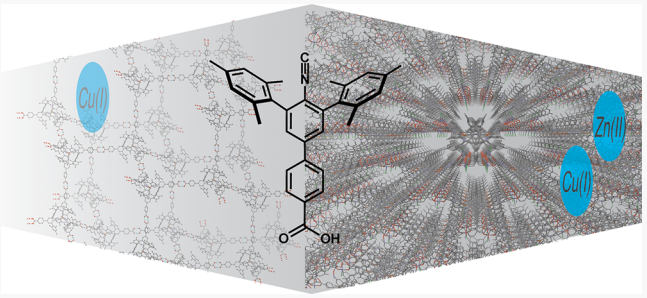

INTRODUCTION

Metal−organic frameworks (MOFs) are a class of three-dimensional, porous crystalline materials that have found application in a variety of areas including catalysis, gas storage, and gas separations.[1−6] Traditionally, MOFs are designed by taking advantage of hard/soft Lewis acid/base theory, where formally oxidized, hard Lewis acidic metal centers are combined with anionic, hard Lewis basic linkers to form strong ionic bonds.[7−10] These ionic metal−ligand interactions can lead to extremely robust frameworks that often possess permanent porosity and high internal surface areas.[4−6,11] However, the reliance on oxidized metal centers for the construction of structural nodes (i.e., secondary building units, SBUs) in these network materials often precludes their direct participation in multielectron redox processes. Such redox behavior is exemplified by low-valent metal centers, which are electronically mismatched with hard, anionic ligands for the purpose of network formation.[12,13] Accordingly, there have been increasing efforts aimed at the preparation of mixed-metal MOFs, where hard Lewis acidic metal centers comprise the structural portion of the network, while "softer", more electron-rich metal centers are appended as reactive sites.[14] Because such materials are finding increasing applications in

Received: June 14, 2021
Published: August 4, 2021

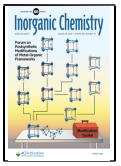

https://doi.org/10.1021/acs.inorgchem.1c01804
Inorg. Chem. 2021, 60, 12545−12554

Scheme 1. Synthesis of the Hetroditopic Isocyanide/Carboxylic Acid TIB^{Mes2}H

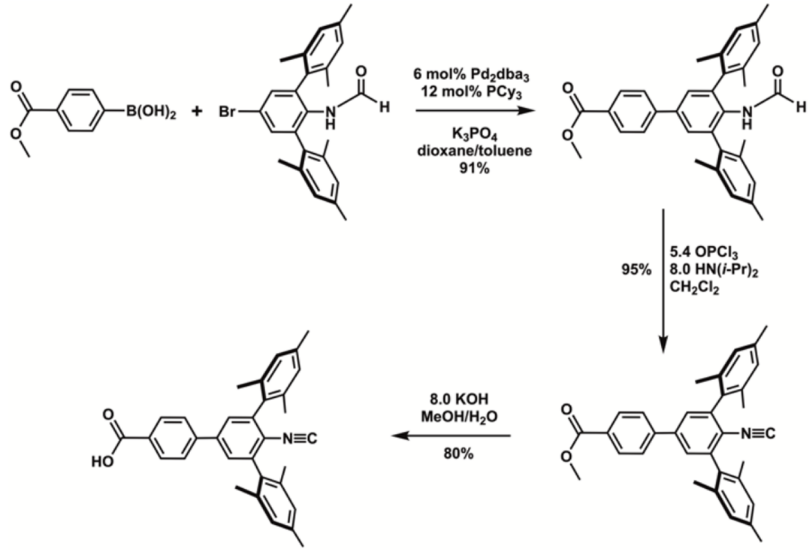

multielectron or tandem/cooperative catalysis,[4,14,15] the development of strategies and methods for their reliable preparation remains desirable.

Several approaches have been reported for the formation of mixed-metal MOFs where low-valent metal centers are a component. Notable among these include postsynthetic metal-ion incorporation into multifunctional linkers,[16,17] metal deposition onto high-valent SBUs,[18−21] and the use of either metalloligands[22−25] or heteroditopic linker groups. Of these strategies, heteroditopic linkers offer unique advantages for the reliable formation of mixed-metal framework materials because two different binding groups can be specifically tuned to match the electronic requirements attendant between hard and soft metal centers. Recently, we introduced ditopic *m*-terphenyl isocyanides [CNAr^{Mes2}]$_2$ and 1,4-(CNAr^{Mes2})$_2$C$_6$H$_4$ [Ar^{Mes2} = 2,6-(2,4,6-Me$_3$C$_6$H$_2$)$_2$C$_6$H$_2$] as linkers for MOF materials.[26−28] Isocyanides are electronically "soft" neutral ligands that function as good σ donors and effective π acids in a manner similar to that of CO.[29,30] While neutral in charge, isocyanides form robust M−L linkages on account of strong π-back-bonding interactions and are therefore adept at stabilizing low-valent metal centers.[13,31−35] As we have previously reported, ditopic *m*-terphenyl isocyanides can be employed for the formation of thermally robust and crystalline organometallic network materials featuring electron-rich metal centers [e.g., Cu(I) and Ni(0)] as structural nodes.[26−28] However, isocyanides are particularly poor ligands for hard metals (e.g., Mg^{2+} and Zn^{2+}) or metals in high formal oxidation states (e.g., Zr^{4+}). Seeking to exploit this disparate coordination behavior, we reasoned that heteroditopic ligands based on an isocyanide and an anionic binding group could offer a uniquely differentiated electronic environment for the formation of mixed-metal network materials. Accordingly, here we report the preparation and use of a heteroditopic isocyanide/carboxylate linker for the formation of robust mixed-metal network materials. In addition, we show that this rigid linker system can also provide hydrogen-bonding networks[36−41] that bridge between molecular and extended-network systems with low-valent metals.

RESULTS AND DISCUSSION

To retain the encumbering steric properties of the *m*-terphenyl isocyanide framework while also introducing a carboxylate group in a rigid, linear topology, we targeted the heteroditopic ligand 1-CNAr^{Mes2}-4-C$_6$H$_4$CO$_2$H (TIB^{Mes2}H; TIB = terphenyl isocyanide benzoate). This linker features a benzoic acid group appended to the para position of the monodentate CNAr^{Mes2} ligand, which has been well utilized for the preparation of low-coordinate, low-valent transition-metal complexes.[42−52] The synthesis of this heterotopic ligand was accomplished by Suzuki coupling of the *p*-bromo-*m*-terphenyl formamide HC(O)NH(*p*-BrAr^{Mes2}), with 4-methoxycarbonylphenylboronic acid to provide the methyl ester-protected heterotopic *m*-terphenyl formamide ligand 1-HC(O)N(H)Ar^{Mes2}-4-C$_6$H$_4$CO$_2$CH$_3$ (Scheme 1). Subsequent dehydration of this formamide afforded the protected isocyanide 1,4-(CNAr^{Mes2})-C$_6$H$_4$CO$_2$CH$_3$ as an off-white solid. The latter was readily deprotected with potassium hydroxide (KOH) to provide the target carboxylic acid TIB^{Mes2}H in 80% yield after an acidic workup (Scheme 1). The isocyanocarboxylic acid TIB^{Mes2}H is isolated as a colorless microcrystalline solid and gives rise to a ν_{CN} stretching band of 2117 cm^{-1} (attenuated-total-reflectance infrared, ATR-IR) and a $^{13}C\{^1H\}$ NMR chemical shift of 170.9 ppm for the isocyanide carbon. These spectroscopic features agree well with previously reported mono- and ditopic *m*-terphenyl isocyanides.[26,28,30] Crystallographic structural determination of TIB^{Mes2}H revealed that it is indeed an asymmetric rigid linear organoisocyanide containing a benzoic acid group. In the solid state, the benzoic acid group is canted ∼33° relative to the Ar^{Mes2} unit (Figure S5.1). This torsion angle is similar to that found between the CNAr^{Mes2} groups and the phenylene spacer in the ditopic isocyanide 1,4-(CNAr^{Mes2})$_2$C$_6$H$_4$,[28] but differs substantially from the solid-state structure of the directly fused ditopic isocyanide [CNAr^{Mes2}],[26] which adopts a nearly coplanar arrangement of its central biphenyl unit.[26] However, it is important to note that one TIB^{Mes2}H packs in a distinct herringbone arrangement in the solid state on account of significant hydrogen bonding between the carboxylic acid groups (Figure S5.2).

To explore the ligation properties of TIB^{Mes2}H and determine whether the isocyanide unit can bind selectively to

https://doi.org/10.1021/acs.inorgchem.1c01804
Inorg. Chem. 2021, 60, 12545−12554

Scheme 2. Coordination Studies of $TIB^{Mes2}H$ with Cu(I) Centers

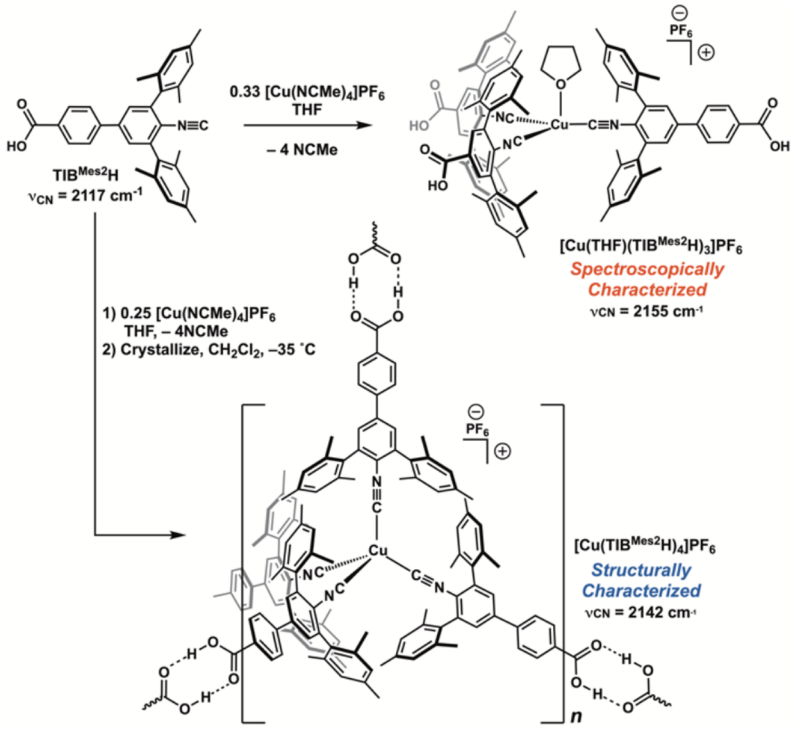

low-valent metals, we surveyed its coordination behavior toward Cu(I) centers. There is a long-standing coordination chemistry of copper(I) isocyanide complexes,[53−55] and they have been utilized by us and others to assess the relative binding abilities of derivatized isocyanide ligands.[42,56−58] While Cu(I) centers are not the most effective π bases, the relatively low 1+ formal oxidation state does not lead to an energetically contracted d-orbital manifold. This feature allows Cu(I) centers to readily bind electronically softer ligands such as isocyanides, phosphines, and thiols, which contrasts with formally Zn(II) centers despite being isoelectronic. However, copper(I) carboxylates are also a well-known class of molecular and network materials,[59−62] thereby providing an ideal test for the ability of a heteroditopic isocyanide/carboxylate ligand for binding selectivity on the basis of electronic differentiation.

The isocyanide unit of TIB^{Mes2} can selectively bind to Cu(I) centers, and the extent of ligation in the resulting complexes can be controlled by steric pressures of the *m*-terphenyl group. For example, the treatment of $TIB^{Mes2}H$ with $[Cu(NCMe)_4]PF_6$ in a 3:1 ratio in a tetrahydrofuran (THF) solution generates a single new product as assayed by ^1H NMR spectroscopy. Importantly, Fourier transform infrared (FTIR) analysis revealed a sharp ν_{CN} band centered at 2155 cm^{-1}. As we have previously shown for both molecular copper(I) tris(isocyanide) complexes[42] and isocyanide networks featuring copper(I) tris(isocyanide) SBUs,[26,28] such a high-energy ν_{CN} band is diagnostic of a cationic $[(L)Cu(CNR)_3]^+$ coordination environment, where the fourth L-type ligand is a weak σ donor. In the presence of stronger σ donors, a distinctive shift of ν_{CN} to lower energy is observed because of greater Cu p-orbital participation in bonding.[28] Unfortunately, despite multiple attempts, single crystals suitable for structural determination from this 3:1 $TIB^{Mes2}H/[Cu(NCMe)_4]PF_6$ reaction could not be obtained. However, circumstantial evidence for the formation of the tris(isocyanide) complex $[(THF)Cu(TIB^{Mes2}H)_3]PF_6$ comes from the reaction of TIB^{Mes2} and $[Cu(NCMe)_4]PF_6$ in a 4:1 ratio (Scheme 2). Analysis of this latter reaction mixture by solution-phase IR spectroscopy resulted in the same 2152 cm^{-1} ν_{CN} band as the reaction employing a 3:1 $TIB^{Mes2}H$/Cu ratio. However, this band was also accompanied by a less intense band at 2118 cm^{-1} indicative of free $TIB^{Mes2}H$. Previously, we showed that the molecular salt $[(THF)Cu(CNAr^{Mes2})_3]OTf$, which features the same *m*-terphenyl unit as that found in TIB^{Mes2}, resists the binding of a fourth isocyanide ligand in solution.[42] Instead, 1:1 $[(THF)Cu(CNAr^{Mes2})_3]OTf/CNAr^{Mes2}$ mixtures establish a rapid isocyanide-exchange equilibrium, as determined by FTIR and ^1H NMR spectroscopy.[42] On account of the similar steric profiles between $TIB^{Mes2}H$ and $CNAr^{Mes2}$, we contend that a similar exchange process is likely established in solution and that the 2155 cm^{-1} ν_{CN} band arises from the tris(isocyanide) complex $[(THF)Cu(TIB^{Mes2}H)_3]PF_6$. Adding further credence to this suggestion is the fact that crystallization of the 4:1 $TIB^{Mes2}H/[Cu(NCMe)_4]PF_6$ mixture from a CH_2Cl_2 solution resulted in colorless single crystals, which were determined to be the tetrakis(isocyanide) complex $[Cu(TIB^{Mes2}H)_4]PF_6$ by X-ray crystallography (Figure 1). Most importantly, ATR-IR analysis of single crystals $[Cu(TIB^{Mes2}H)_4]PF_6$ gave rise to a ν_{CN} band of 2142 cm^{-1}, which is shifted to lower energy relative to $[(THF)Cu(TIB^{Mes2}H)_3]PF_6$ because of the presence of a fourth isocyanide ligand with moderate σ-donating properties.

Whereas the structure of $[Cu(TIB^{Mes2}H)_4]PF_6$ confirms that the isocyanide unit selectively binds to the Cu(I) center, it also provides a rationalization for the isolation of a tetrakis(isocyanide) complex in the solid state. Inspection of the extended structure of $[Cu(TIB^{Mes2}H)_4]PF_6$ reveals that it is organized into a 7-fold-interpenetrated diamondoid (**dia**) hydrogen-bonding network (Figure 2). As shown in Figure 2, the free carboxylic acid groups of the coordinated $TIB^{Mes2}H$

https://doi.org/10.1021/acs.inorgchem.1c01804
Inorg. Chem. 2021, 60, 12545−12554

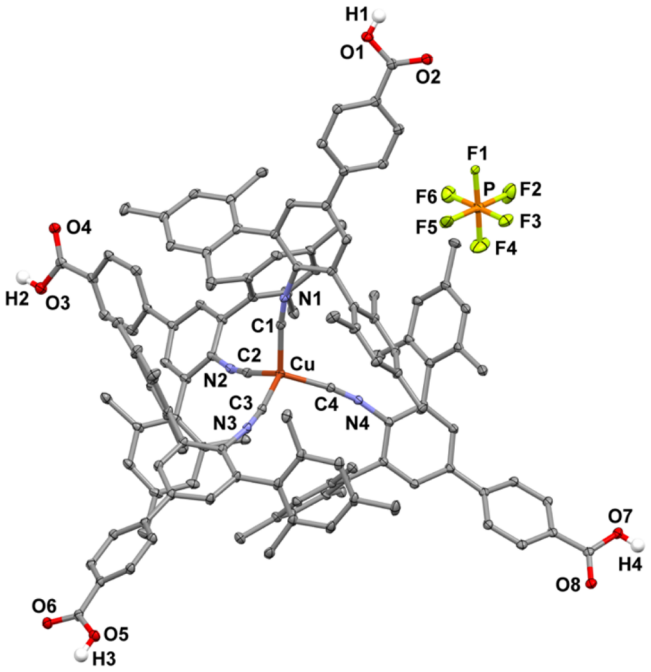

Figure 1. Structure of the molecular core of the hydrogen-bonded network $[Cu(TIB^{Mes2}H)_4]PF_6$. H atoms other than those on the carboxylate groups and solvent molecules of cocrystallization have been omitted for clarity.

ligand form $R_2^2(8)$ hydrogen bonds[63] to nearest-neighbor $[Cu(TIB^{Mes2}H)_4]^+$ units. This extended lattice structure reasonably stabilizes the coordination of a fourth isocyanide ligand in a manner that overcomes the attendant steric pressures between the *m*-terphenyl groups. Notably, we have observed this effect previously in the isocyanide coordination network Cu-^{ISO}CN-1, which features the ditopic isocyanide $[CNAr^{Mes2}]_2$.[26] In Cu-^{ISO}CN-1, the formation of an extended lattice similarly stabilizes tetrahedral $[Cu(CNAr^{Mes2})_4]^+$ cores by inhibiting ligand dissociation. For the hydrogen-bonding network formed by $[Cu(TIB^{Mes2}H)_4]PF_6$, the 7-fold-interpenetrated **dia** net results in a densely packed lattice lacking significant voids. Close inspection of the lattice reveals the presence of ca. 16.5 × 16.1 Å rectangular channels along the crystallographic *b* axis, which is occupied by the $[PF_6]^-$ ions as well as CH_2Cl_2 molecules of cocrystallization (Figure 2). Notably, this dense packing of hydrophobic *m*-terphenyl units results in good stability toward liquid water. Indeed, $[Cu(TIB^{Mes2}H)_4]PF_6$ can be suspended in water for 24 h without appreciable degradation, as assayed by ATR-IR spectroscopy (Figure S2.8). This dense packing also protects the Cu(I) centers in $[Cu(TIB^{Mes2})_4]PF_6$ from oxidation because it is indefinitely stable as a solid on the benchtop. However, the hydrogen-bonding network is readily disrupted by polar organic solvents such as THF, in which dissolution is rapid and an equilibrium between a copper(I) tris(isocyanide) complex and free $TIB^{Mes2}H$ is quickly reestablished. Thermogravimetric analysis (TGA) of crystalline $[Cu(TIB^{Mes2}H)_4]PF_6$ revealed a persistent multistage decomposition between 150 and 500 °C (Figure S4.1) rather than a well-defined process indicative of desolvation, followed by single-step decomposition. Hydrogen-bonding networks, especially those utilizing T_d-symmetric building blocks, are known to display robust thermal behavior as solids.[40] In contrast, the ill-defined thermal behavior of $[Cu(TIB^{Mes2}H)_4]PF_6$ likely reflects an inherent steric instability posed by the *m*-terphenyl groups that is not overcome by the totality of hydrogen bonding at elevated temperatures.

With the selectivity of the $TIB^{Mes2}H$ isocyanide unit for Cu(I) centers established, the ability of the carboxylate group to bind a second metal center was assessed for the purpose of mixed-metal MOF formation. To ensure that electronic differentiation could be achieved, hard Lewis acidic Zn(II) centers were investigated for preferential binding with the TIB^{Mes2} carboxylate unit. Most notably, preligation of the $TIB^{Mes2}H$ isocyanide group to Cu(I), followed by deprotonation of the free carboxylic acid group prior to the introduction of a Zn(II) source, served as a reliable strategy for the formation of mixed-metal frameworks (Scheme 3). For example, stirring of a 3:1 mixture of $TIB^{Mes2}H$ and [Cu-

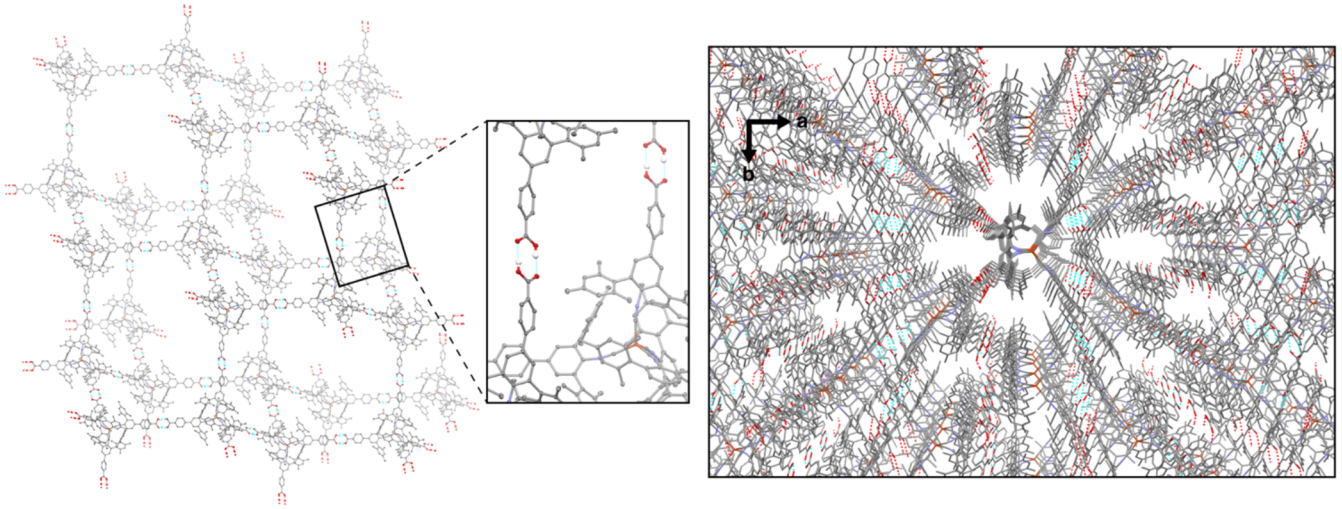

Figure 2. (Left) Perspective view of the diamondoid net of $[Cu(TIB^{Mes2}H)_4]PF_6$ with 7-fold interpenetration removed for clarity. The inset depicts a zoomed view of $R_2^2(8)$ hydrogen bonds that assemble the hydrogen-bonding network. (Right) Full interpenetrated view of $[Cu(TIB^{Mes2}H)_4]PF_6$ down the crystallographic *b* axis showing an internal channel structure. CH_2Cl_2 solvent molecules of cocrystallization and $[PF_6]^-$ ions present within the channels have been omitted for clarity.

https://doi.org/10.1021/acs.inorgchem.1c01804
Inorg. Chem. 2021, 60, 12545−12554

Scheme 3. Synthesis of the Mixed-Metal Framework Cu/Zn-^{ISO}CN-5

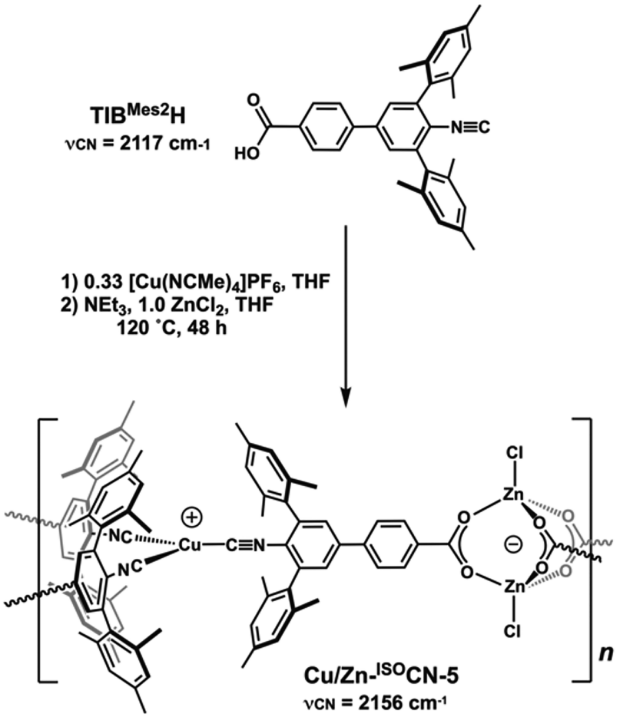

$(NCMe)_4]PF_6$ for 30 min in a THF solution, followed by the addition of NEt_3 (3.0 equiv), results in ^{1}H NMR and FTIR spectra consistent with carboxylate deprotonation but retention of a copper(I) tris(isocyanide) core (Figure S2.11). The treatment of this THF mixture with $ZnCl_2$, followed by solvothermal heating at 120 °C for 48 h, resulted in the deposition of large, colorless cubic-shaped single crystals. Crystallographic structural determination revealed these crystals to be a mixed-metal Cu(I)/Zn(II) framework (denoted as Cu/Zn-^{ISO}CN-5) that possesses a highly unusual zwitterionic repeat unit. As shown in Figure 3, the carboxylate unit of TIB^{Mes2} is competent for the binding of Zn(II), while three ligands assemble into a dimeric $[Cl_2Zn(O_2CR)_3]^-$ paddlewheel that possesses terminal chloride ligands and an overall negative charge. This Zn_2-based SBU is charge-balanced by an unsolvated $[Cu(CNR)_3]^+$ cation that adopts a perfect trigonal-planar coordination geometry [$\sum\angle$(C−Cu−C) = 359.99(1)°]. Importantly, residuals within the electron density map of Cu/Zn-^{ISO}CN-5 do not indicate the presence of either $[PF_6]^-$ anions or triethylammonium cations, thereby providing additional evidence for a zwitterionic formulation between the Cu- and Zn-based SBUs.

It is important to note that the synthesis of Cu/Zn-^{ISO}CN-5 can be viewed as a variant of the metalloligand approach for accessing mixed-metal MOFs.[22−24] Whereas the vast majority of metalloligands contain a multidentate chelating unit to sequester the first metal and a free carboxylate to bind a second metal, preligation of three monodentate TIB^{Mes2}H ligands to Cu(I) achieves the same effect on account of electronic differentiation between isocyanide and carboxylate donor groups. This latter approach is further validated by inductively coupled plasma mass spectrometry analysis on digested Cu/Zn-^{ISO}CN-5, which resulted in an observed ^{63}Cu/^{66}Zn concentration ratio of 1:2 and is fully consistent with both the structural motifs present in the solid state and their specific charge-balancing requirements. Furthermore, the ATR-IR spectrum of crystalline Cu/Zn-^{ISO}CN-5 revealed a sharp ν_{CN} band at 2156 cm^{-1}, which provides additional evidence for the presence of a nonpyramidalized $[Cu(CNR)_3]^+$ node within Cu/Zn-^{ISO}CN-5.[28] To this end, dissolution of the hydrogen-bonding network $[Cu(TIB^{Mes2}H)_4]PF_6$ in THF, followed by the addition of NEt_3 and $ZnCl_2$, also produces Cu/Zn-^{ISO}CN-5 after solvothermal heating, as assayed by both single-crystal and powder X-ray diffraction (SCXRD and PXRD). As suggested from the solution-phase FTIR data of $[Cu(TIB^{Mes2}H)_4]PF_6$, dissociation of a TIB^{Mes2} ligand more than likely generates a tris(isocyanide) core that engages with other metal centers through carboxylate units after deprotonation.

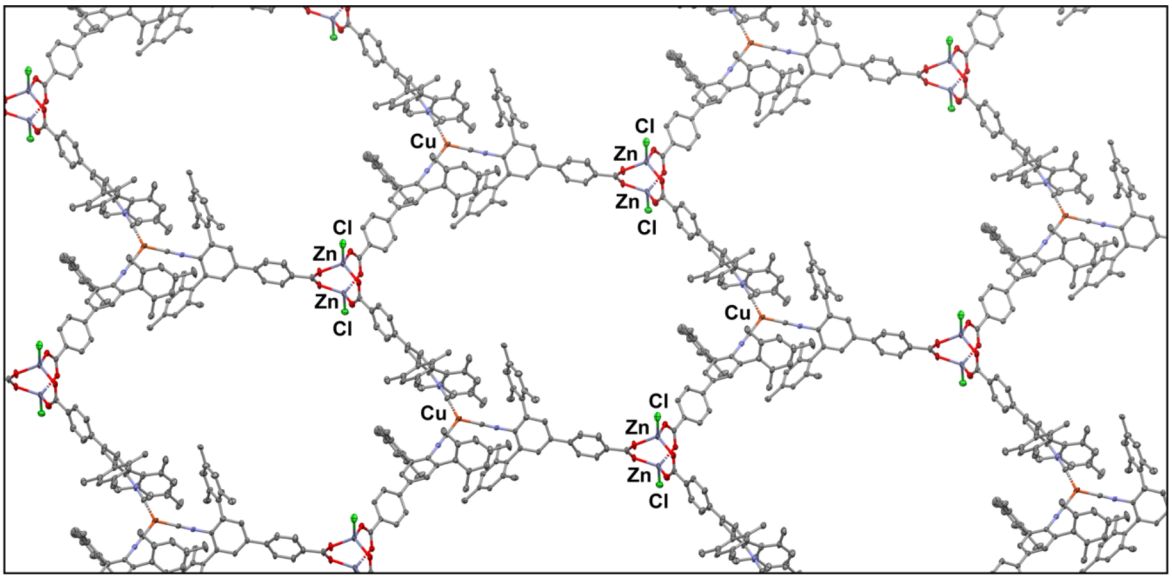

Figure 3. Solid-state structure of one hexagonal (3,3) **hbc** net layer of Cu/Zn-^{ISO}CN-5 showing cationic $[Cu(CNR)_3]^+$ and anionic $[Cl_2Zn_2(O_2CR)_3]^-$ SBUs.

https://doi.org/10.1021/acs.inorgchem.1c01804
Inorg. Chem. 2021, 60, 12545−12554

Inspection of the extended solid-state structure of Cu/Zn-^{ISO}CN-5 revealed that the Cu(I)/Zn(II) dual SBUs organize into an AB-stacked-layer, two-dimensional (3,3) honeycomb (**hcb**) network in the *Fdd*2 space group (Figure 4). Despite possessing ca. 32 Å hexagonal apertures, the layers

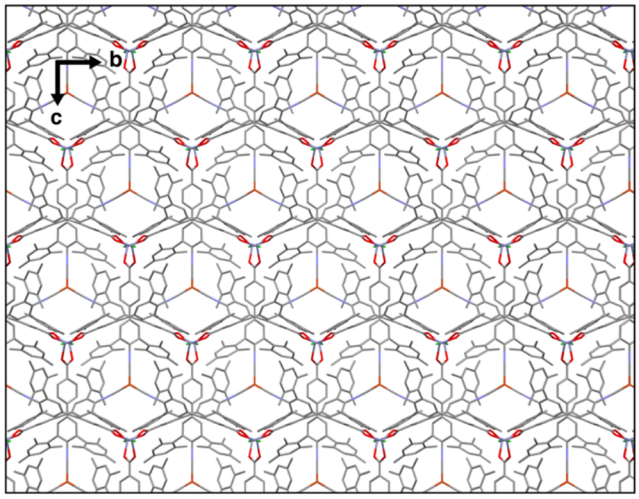

Figure 4. View of Cu/Zn-^{ISO}CN-5 along the crystallographic *a* axis depicting a noninterpenetrated AB-stacked-layer arrangement of two-dimensional (3,3) **hbc** nets.

are not interpenetrated. However, close stacking of the 2D layers, which is fostered by van der Waals contacts between the *m*-terphenyl groups, creates an overall densely packed material that exhibits good thermal stability. TGA on a single-crystalline sample of Cu/Zn-^{ISO}CN-5 resulted in a well-behaved, single-step decomposition with an onset temperature of 310 °C. This thermal behavior contrasts significantly with that of the hydrogen-bonding network $[Cu(TIB^{Mes2}H)_4]PF_6$ and indicates that increased thermal stability can be achieved for metal isocyanide nodes by SBU formation at the carboxylate groups.

Whereas Cu/Zn-^{ISO}CN-5 exists in the solid state as a densely packed layered material, there are narrow (19 Å × 17 Å)-wide channels that transverse the diagonal between the crystallographic *a* and *c* axes (Figure 5). Notably, the trigonal-planar $[Cu(CNR)]^+$ SBUs run parallel to these channels, as does one terminal chloride ligand of the Zn paddlewheel nodes. While this particular lattice arrangement suggests that exogenous substrates can potentially access the coordinatively unsaturated Cu(I) centers, the small diameter of these channels, coupled with the relatively large van der Waals radii of Cl atoms, is likely to present significant steric restrictions on substrate penetration. Indeed, this notion was confirmed by gas sorption measurements of Cu/Zn-^{ISO}CN-5 samples activated at 115 °C. Attempted measurement of the N_2 sorption isotherms showed negligible uptake and the corresponding surface area. However, CO_2 sorption runs resulted in modest uptake and derived Brunauer–Emmett–Teller and Langmuir surface area values of 141 and 191 m^2/g, respectively. Accordingly, we presume that the increased polarizability of CO_2 enables access to the narrow hydrophobic channels present in Cu/Zn-^{ISO}CN-5. To this end, O_2 sorption measurements on Cu/Zn-^{ISO}CN-5 also resulted in negligible uptake, despite the presence of low-valent and coordinatively unsaturated $[Cu(CNAr)_3]^+$ sites along the channel walls. This was corroborated by ATR-IR spectroscopic analysis, which

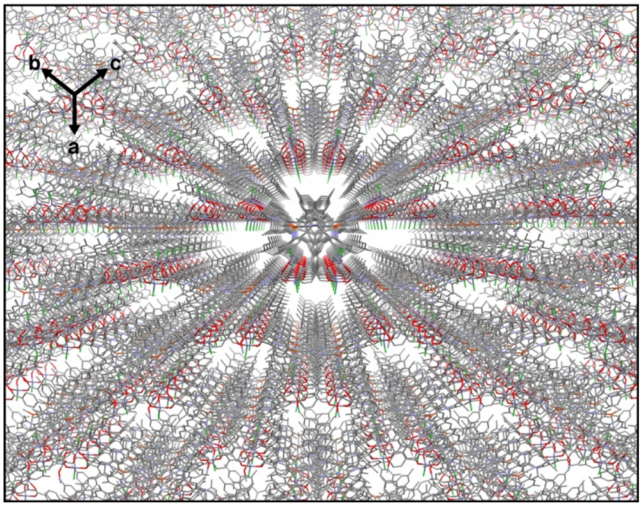

Figure 5. Channel structure of Cu/Zn-^{ISO}CN-5 along the diagonal between the crystallographic *a* and *c* axes. Chloride ligands of the Zn_2 SBU are colored in green and are found to line the channels.

showed no change in the ν_{CN} band after dosing single-crystalline Cu/Zn-^{ISO}CN-5 with 1 atm of O_2 for 24 h. While this latter observation may indicate a resistance of the Cu centers to either oxidation or O_2 binding that is electronic in origin, we currently favor the presence of an inaccessible channel structure within Cu/Zn-^{ISO}CN-5 as an explanation for this lack of reactivity.

As indicated from its chemical resistance to O_2, Cu-^{ISO}CN-5 displays excellent air stability. Crystalline samples of the material were subjected to drying under vacuum for 15 min and were indefinitely stable to ambient atmospheric conditions on the benchtop. Over the course of 2 weeks, intermittent ATR-IR spectroscopic analysis showed no change in the ν_{CN} or the ν_{CO} bands of Cu-^{ISO}CN-5, and no indication of free $TIB^{Mes2}H$ was observed that would indicate decomposition of the Cu(I) center. PXRD analysis of the sample also showed no loss in crystallinity over the course of 2 weeks, indicating good stability of the framework to atmospheric conditions (Figure S2.13). However, while Cu-^{ISO}CN-5 displays excellent stability in air, addition of the material to deionized water resulted in a loss in crystallinity over the course of 24 h (Figure S5.8). ATR-IR spectroscopic analysis revealed a broadening of the isocyanide stretch, in addition to a distinct red shift of the carboxylate ν_{CO} stretch to 1608 cm^{-1} from 1629 cm^{-1} (Figure S2.12). Accordingly, this loss in crystallinity is likely due to hydrolysis of the metal carboxylate SBU, which is common for zinc carboxylate paddlewheel-based MOFs.[64,65]

CONCLUSIONS

The development of synthetic methods that can reliably incorporate low-valent metals into network materials remains attractive as a means of enhancing the physical and chemical properties of porous solids. In addition, the preparation of mixed-metal networks, where the electronic attributes of two or more metals are complementary, are finding increased utilization in the area of catalysis and separations chemistry.[14,15] Here, we demonstrate that two different donor groups within an electronically differentiated heteroditopic ligand can be used to assemble a mixed-metal MOF that incorporates low-valent metal sites in a predictable and selective fashion. Specifically, the heteroditopic isocyanide/

https://doi.org/10.1021/acs.inorgchem.1c01804
Inorg. Chem. 2021, 60, 12545–12554

carboxylic acid ligand $TIB^{Mes2}H$ can selectively bind low-valent Cu(I) centers through the isocyanide unit, while leaving the carboxylic acid group unperturbed. Without further elaboration, the free carboxylic acid in $Cu(I)/TIB^{Mes2}H$ complexes allows for the formation of solid-state hydrogen-bonding networks. However, upon deprotonation, the resulting carboxylate can bind to a "hard" Zn(II) center and enable the formation of a mixed-metal framework material. Whereas the encumbering steric properties of the *m*-terphenyl group of the TIB^{Mes2} linker enable the incorporation of coordinatively unsaturated $[CuL_3]^+$ sites within this Cu(I)/Zn(II) framework, its densely packed AB layer structure does not result in significant porosity or surface area. However, given the wide range of carboxylate-based SBUs that give rise to permanently porous three-dimensional framework materials,[7,8] we believe this approach can be effective for the reliable incorporation of low-valent, as well as coordinatively unsaturated, metal centers. Accordingly, synthetic investigations seeking to expand the use of TIB^{Mes2} and related heteroditopic linkers for this purpose are in progress.

EXPERIMENTAL SECTION

General Considerations. Unless otherwise stated, all manipulations were performed under an atmosphere of dry N_2 using standard Schlenk and glovebox techniques. Solvents were dried and degassed according to standard procedures.[66] Unless otherwise stated, reagent-grade starting materials were purchased from commercial sources and purified where necessary according to standard procedures.[67] The *p*-bromoaniline H_2NAr^{Mes2}-*p*-Br was prepared as previously reported.[26] Solution ^1H and $^{13}C\{^1H\}$ NMR were recorded on a Bruker 300, Varian 400, Varian X-Sens 500, or JEOL ECA-500 spectrometer. ^1H and $^{13}C\{^1H\}$ NMR chemical shifts are reported in parts per million relative to $SiMe_4$ (^1H and $^{13}C\{^1H\}$, δ = 0.0 ppm) with reference to residual proton resonances of δ = 7.16 ppm (^1H, C_6D_6) and δ = 7.26 ppm (^1H, $CDCl_3$).[68] ^{19}F NMR spectra were referenced externally to neat trifluoroacetic acid, $F_3CC(O)OH$ (δ = −78.5 ppm vs δ = 0.0 ppm for $CFCl_3$). Solid-state IR spectra were collected at 2 cm^{-1} resolution as either KBr pellets or using a Bruker Platinum Alpha ATR-IR spectrometer equipped with a diamond crystal. The following abbreviations are used to describe the intensity and characteristics of important IR absorption bands: vs = very strong, s = strong, m = medium, w = weak, vw = very weak, b = broad, vb = very broad, and sh = shoulder. Samples for PXRD were mounted on nylon loops with minimal Paratone oil and analyzed at 300 K under a N_2 stream using Cu Kα radiation (λ = 1.54178 Å) on a Bruker Kappa diffractometer equipped with a VÅNTEC-500 area detector and an Oxford Cryostream 700. High-resolution mass spectrometry (HR-MS) was recorded at the UCSD Molecular Mass Spectrometry Facility using an Agilent 6230 Accurate-Mass TOFMS spectrometer running in either a positive- or negative-ion mode.

Synthesis of HC(O)NH(p-BrAr^{Mes2}). Formic acid (3.41g, 74 mmol, 10 equiv) was added dropwise via a syringe to stirring acetic anhydride (6.04 g, 59.2 mmol, 8.0 equiv). The mixture was warmed to 50 °C for 1 h to generate formyl acetic anhydride. This mixture was allowed to cool and then transferred to a stirring THF solution of H_2NAr^{Mes2}-*p*-Br (3.0 g, 7.4 mmol). This mixture was stirred for 24 h, after which all volatiles were removed by dynamic vacuum at 50 °C to yield $HC(O)NH(p\text{-}BrAr^{Mes2})$ as a colorless solid that was used without further purification. Yield: 3.06 g, 7.03 mmol, 95%. ^1H NMR (300.1 MHz, $CDCl_3$, 20 °C): δ 7.60 (d, 1H, J = 9 Hz, NHC(O)*H*), 7.29 (s, 2H, *m*-Ar), 6.94 (s, 4H, *m*-Mes), 6.53 (d, 1H, J = 9 Hz, N*H*C(O)H), 2.30 (s, 6 H, (Mes-*p*-CH_3)), 2.02 (s, 12H, (Mes-*o*-CH_3)). $^{13}C\{^1H\}$ NMR (125.7 MHz, $CDCl_3$, 20 °C): δ 162.5 (*H*C(O)N), 138.5, 135.7, 135.3, 133.2, 132.9, 131.8, 129.1, 118.8, 21.2 (*p*-Mes-CH_3), 20.5 (*o*-Mes-CH_3). FTIR-ATR (diamond surface, 20 °C): ν_{CO} 1690 cm^{-1} (s), ν_{NH} 3189 (w), also 2917 (m), 1660 (s), 1521 (s), 1380 (w), 1027 (m), 839(s), 694 (w) cm^{-1}. HR-MS (ESI-TOFMS, positive-ion mode). Predicted for $C_{25}H_{26}BrNO$: m/z 435.1198. Found: m/z 436.1266 ($[M + H]^+$).

Synthesis of 1-HC(O)N(H)Ar^{Mes2}-4-$C_6H_4CO_2CH_3$. A resealable ampule was charged with the formamide $HC(O)NH(p\text{-}BrAr^{Mes2})$ (0.480 g, 1.10 mmol), Pd_2dba_3 (0.030 g, 0.032 mmol, 3 mol %), PCy_3 (0.019 g, 0.064 mmol, 6 mol %), K_3PO_4 (0.933 g, 4.39 mmol, 4.0 equiv), and 4-(methoxycarbonyl)phenylboronic acid (0.198 g, 1.10 mmol, 1.0 equiv). 1,4-Dioxane (25 mL) and toluene (8 mL) were used to dissolve the solids. The reaction mixture was stirred at 75 °C for 24 h under an atmosphere of N_2. The mixture was cooled and filtered through a medium-porosity fritted funnel packed with silica, and the filter cake was washed with CH_2Cl_2 (3 × 15 mL). The filtered crude mixture was stripped of all volatiles, washed and sonicated with cold hexanes, and then filtered. The resulting colorless solid, 1-$HC(O)N(H)Ar^{Mes2}$-4-$C_6H_4CO_2CH_3$, was used without further purification. Yield: 0.495 g, 1.01 mmol, 91%. ^1H NMR (300.1 MHz, $CDCl_3$, 20 °C): δ 8.09 (d, 2H, J = 8.4 Hz, C_6H_4), 7.70 (d, 1H, J = 9.4 Hz, NHC(O)*H*), 7.69 (d, 2H, J = 8.4 Hz, C_6H_4), 7.45 (s, 2H, *m*-Ar), 6.99 (s, 4H, *m*-Mes), 6.67 (d, 1H, J = 9.1 Hz, N*H*C(O)H), 3.93 (s, 3H, C(O)OCH_3), 2.34 (s, 6 H, Mes-*p*-CH_3), 2.07 (s, 12H, Mes-*o*-CH_3). $^{13}C\{^1H\}$ NMR (125.7 MHz, $CDCl_3$, 20 °C): δ 167.0 (*H*C(O)N), 162.5 (*C*(O)OCH_3), 144.03, 138.4, 137.2, 135.9, 134.2, 133.7, 132.5, 130.3, 129.2, 128.9, 126.8, 53.3 (COOCH_3), 21.2 (Mes-*p*-CH_3), 20.5 (Mes-*o*-CH_3). FTIR-ATR (diamond surface, 20 °C): $\nu_{CO(ester)}$ 1720, $\nu_{CO(formamide)}$ 1685 (s), ν_{NH} 3368 (w), also 2913 (m), 1606 (s), 1271 (s), 1098 (s), 962 (w), 851(s), 752 (w) cm^{-1}. HR-MS (ESI-TOFMS, positive-ion mode). Predicted for $C_{33}H_{33}NO_3$: m/z 491.2460. Found: m/z 492.2533 ($[M + H]^+$).

Synthesis of 1,4-(CNAr^{Mes2})$C_6H_4CO_2CH_3$. To a stirring CH_2Cl_2 solution of 1-$HC(O)N(H)Ar^{Mes2}$-4-$C_6H_4CO_2CH_3$ (0.500 g, 1.02 mmol) was added diisopropylamine (0.82 g, 8.1 mmol, 8 equiv) via a syringe. After stirring for 5 min, $POCl_3$ (0.84 g, 5.49 mmol, 5.4 equiv) was added dropwise via a syringe and the solution was stirred for 24 h. Aqueous Na_2CO_3 (1.5 M, 50 mL) was added, and the resulting mixture was stirred for 5 h. The organic and aqueous layers were then separated, and the organic layer was washed with deionized water. The aqueous layers were combined and extracted with 3 × 25 mL of CH_2Cl_2. The organic extracts were combined, dried over $MgSO_4$, and filtered and volatiles were removed under reduced pressure. The resultant solid was washed with cold hexanes, collected by filtration, and dried under reduced pressure. Yield: 0.460 g, 0.970 mmol, 95%. ^1H NMR (300.1 MHz, $CDCl_3$, 20 °C): δ 8.11 (d, 2H, J = 8.4 Hz, C_6H_4), 7.68 (d, 2H, J = 8.5 Hz, C_6H_4), 7.51 (s, 2H, *m*-Ar), 7.00 (s, 4H, *m*-Mes), 3.94 (s, 3H, COOCH_3), 2.34 (s, 6 H, Mes-*p*-CH_3), 2.08 (s, 12H, Mes-*o*-CH_3). $^{13}C\{^1H\}$ NMR (125.7 MHz, $CDCl_3$, 20 °C): δ 168.2 (*C*N), 167.1 (*C*(O)OMe), 143.8, 141.2, 140.4, 138.4, 135.9, 134.2, 130.7, 130.1, 128.9, 128.2, 127.5, 52.7 (C(O)OCH_3), 21.6 (Mes-*p*-CH_3), 20.6 (Mes-*o*-CH_3). FTIR-ATR (diamond surface, 20 °C): ν_{CN} 2117 (s), ν_{CO} 1723 (s), also 2920 (m), 1611 (s), 1434 (m), 1277 (s), 1105 (s), 852(s), 774 (s) cm^{-1}. HR-MS (ESI-TOFMS, positive-ion mode). Predicted for $C_{33}H_{31}NO_2$: m/z 473.2455. Found: m/z 474.2424 ($[M + H]^+$).

Synthesis of 1,4-(CNAr^{Mes2})$C_6H_4CO_2H$ (TIB^{Mes2}H). KOH (0.152 g, 2.71 mmol, 8.0 equiv) was dissolved in a 1:1 mixture of methanol and deionized water. The mixture was degassed and transferred to a stirring THF solution of 1,4-(CNAr^{Mes2})$C_6H_4CO_2CH_3$ (0.160 g, 0.338 mmol). This mixture was stirred at 50 °C for 15 h under an atmosphere of N_2. Upon cooling, all volatiles were removed under dynamic vacuum to yield a solid product. The resulting solid was washed with 1.0 M HCl (3 × 10 mL), followed by a rinse with cold hexanes and drying under reduced pressure. Yield: 0.125 g, 0.272 mmol, 80%. ^1H NMR (500.2 MHz, $CDCl_3$, 20 °C): δ 8.18 (d, 2H, J = 8.1 Hz, C_6H_4), 7.72 (d, 2H, J = 8.1 Hz, C_6H_4), 7.53 (s, 2H, *m*-Ar), 7.00 (s, 4H, *m*-Mes), 2.34 (s, 6 H, Mes-*p*-CH_3), 2.08 (s, 12H, Mes-*o*-CH_3). $^{13}C\{^1H\}$ NMR (125.8 MHz, $CDCl_3$, 20 °C): δ 170.9 (*C*N + *C*(O)OMe), 144.2, 140.6, 140.1, 138.0, 135.5, 133.7, 130.8, 128.7, 128.4, 127.9, 127.1, 125.5, 21.3 (Mes-*p*-CH_3), 20.4 (Mes-*o*-CH_3). ATR-IR (diamond surface, 20 °C): ν_{CN} 2117 (s), ν_{CO} 1692 (s), also 2917 (m), 1609 (s), 1438 (m), 1277(s), 1017 (m), 907 (w), 849 (s),

https://doi.org/10.1021/acs.inorgchem.1c01804
Inorg. Chem. 2021, 60, 12545−12554

770 (s) cm^{-1}. HR-MS (ESI-TOFMS, negative-ion mode). Predicted for $C_{32}H_{29}NO_2$: m/z 459.2198. Found: m/z 458.2137 ($[M - H]^-$).

Synthesis of [Cu(THF)(TIB^{Mes2})$_3$]PF$_6$. A THF solution containing TIB^{Mes2}H (0.040 g, 0.087 mmol, 3.0 equiv) was added to a stirring THF solution containing $[Cu(NCMe)_4]PF_6$ (0.011 g, 0.030 mmol, 1.0 equiv). The reaction mixture was allowed to stir for 15 min, after which all volatiles were removed under reduced pressure. Dissolution of the resulting colorless powder in fluorobenzene, followed by filtration and storage at room temperature for 24 h, resulted in a colorless microcrystalline powder that was collected and dried in vacuo. Yield: 0.031 g, 0.019 mmol, 60%. ^{1}H NMR (499.8 MHz, CD_2Cl_2, 20 °C): δ 8.21 (d, 2H, J = 8.5 Hz), 7.79 (d, 2H, J = 8.5 Hz), 7.59 (s, 2H, *m*-Ar), 6.93 (s, 4H, *m*-Mes), 3.65 (m, 4H, THF), 2.29 (s, 6H, Mes-*p*-CH_3), 2.00 (s, 12H, Mes-*o*-CH_3), 1.82 (m, 4H, THF). ^{13}C{^{1}H} NMR (125.7 MHz, CD_2Cl_2, 20 °C): δ 171.0 (CN), 148.99, 141.0, 139.2, 136.2, 131.5, 129.3, 128.1, 68.6 (THF), 27.0 (Mes-*p*-CH_3), 22.4 (THF), 20.7 (Mes-*o*-CH_3). ^{19}F NMR (376.3 MHz, CD_2Cl_2, 20 °C): δ −73.5 (d, $^1J_{FP}$ = 710.7 Hz). FTIR-ATR (diamond surface, 20 °C, powder sample): ν_{CN} 2155 (s), also ν_{CO} 1720 (s), 1689 (s), 1610 (s), 1419 (m), 1244 (m), 835 (s), 555 (s) cm^{-1}.

Synthesis of [Cu(TIB^{Mes2}H)$_4$]PF$_6$. A THF solution containing TIB^{Mes2} (0.050 g, 0.110 mmol, 4.0 equiv) was added to a stirring THF solution containing $[Cu(NCMe)_4]PF_6$ (0.010 g, 0.025 mmol, 1.0 equiv). The reaction mixture was allowed to stir for 15 min, after which all volatiles were removed under reduced pressure. Dissolution of the resulting colorless powder in CH_2Cl_2, followed by filtration and storage at room temperature for 24 h, resulted in colorless single crystals that were collected and dried in vacuo. Yield: 0.010 g, 0.015 mmol, 59%. FTIR-ATR (diamond surface, 20 °C, crystalline sample): ν_{CN} 2142 (s), also ν_{CO} 1718 (s), 1984 (s), 1610 (s), 1244 (m), 852(s), 776 (s), 494 (s) cm^{-1}. Dissoluton of $[Cu(TIB^{Mes2})_4]PF_6$ in CD_2Cl_2 resulted in spectroscopic signatures indicative of the product resulting from a 3:1 Cu/TIB^{Mes2} mixture and free TIB^{Mes2}.

Synthesis of Cu/Zn-^{ISO}CN-5. A THF solution containing TIB^{Mes2}H (0.015 g, 0.033 mmol, 3.0 equiv) was added to a stirring THF solution containing $[Cu(MeCN)_4]PF_6$ (0.004 g, 0.011 mmol, 1.1 equiv). Triethylamine (6.0 μL, 0.044 mmol, 4.0 equiv) was then added and allowed to stir for 10 min. $ZnCl_2$ (0.0044 g, 0.032 mmol, 3.0 equiv) was dissolved in 1.5 mL of THF and added to this mixture. Upon addition, a white solid formed and was transferred to a 15 mL pressure tube. The solid was heated at 120 °C for 12 h and cooled to 40 °C over the course of 48 h. Colorless single crystals formed on the bottom of the pressure tube, which were washed with 3 × 3 mL of THF and then collected. Yield: 0.008 g, 0.009 mmol (based on the Cu-based repeat unit), 80%. FTIR-ATR (diamond surface, 20 °C): ν_{CN} 2156 (s), also ν_{CO} 1716 (s), 1610 (s), 1244 (m), 778 (s), 557 (s) cm^{-1}.

Crystallographic Structure Determinations. Single-crystal X-ray structure determinations were carried out at low temperature (100 K) on Platform diffractometers equipped with Cu Kα radiation sources and Bruker APEX II detectors. All structures were solved by direct methods with *SHELXS*[69,70] and refined by full-matrix least-squares procedures utilizing *SHELXL* within the *Olex2* small-molecule solution, refinement, and analysis software package.[71] Full details of crystallographic data collection and refinement can be found in the Supporting Information.

■ ASSOCIATED CONTENT

Supporting Information

The Supporting Information is available free of charge at https://pubs.acs.org/doi/10.1021/acs.inorgchem.1c01804.

Representative spectra, physical measurements, and the results of SCXRD and PXRD measurements (PDF)

Accession Codes

CCDC 2085631−2085633 contain the supplementary crystallographic data for this paper. These data can be obtained free of charge via www.ccdc.cam.ac.uk/data_request/cif, or by emailing data_request@ccdc.cam.ac.uk, or by contacting The Cambridge Crystallographic Data Centre, 12 Union Road, Cambridge CB2 1EZ, UK; fax: +44 1223 336033.

■ AUTHOR INFORMATION

Corresponding Author

Joshua S. Figueroa − *Department of Chemistry and Biochemistry, University of California, San Diego, La Jolla, California 92093-0358, United States;* orcid.org/0000-0003-2099-5984; Email: jsfig@ucsd.edu

Authors

Krista P. Balto − *Department of Chemistry and Biochemistry, University of California, San Diego, La Jolla, California 92093-0358, United States*

Milan Gembicky − *Department of Chemistry and Biochemistry, University of California, San Diego, La Jolla, California 92093-0358, United States*

Arnold L. Rheingold − *Department of Chemistry and Biochemistry, University of California, San Diego, La Jolla, California 92093-0358, United States;* orcid.org/0000-0003-4472-8127

Complete contact information is available at: https://pubs.acs.org/10.1021/acs.inorgchem.1c01804

Notes

The authors declare no competing financial interest.

■ ACKNOWLEDGMENTS

We are grateful to the National Science Foundation (Grant DMR-2106713) for support of this work. This work was additionally sponsored in part by the University of California, San Diego, Materials Research Science and Engineering Center (UCSD MRSEC), supported by the National Science Foundation (Grant DMR-2011924). The use of facilities and instrumentation supported by the National Science Foundation through the UCSD MRSEC is also gratefully acknowledged. We thank Brandon R. Barnett and R. Erik Sikma for assistance with gas sorption measurements and helpful discussions.

■ REFERENCES

(1) Lee, J.; Farha, O. K.; Roberts, J.; Scheidt, K. A.; Nguyen, S. T.; Hupp, J. T. Metal−organic Framework Materials as Catalysts. *Chem. Soc. Rev.* **2009**, *38*, 1450−1459.

(2) Li, J.-R.; Kuppler, R. J.; Zhou, H.-C. Selective Gas Adsorption and Separation in Metal−Organic Frameworks. *Chem. Soc. Rev.* **2009**, *38*, 1477−1504.

(3) Li, H.; Wang, K.; Sun, Y.; Lollar, C. T.; Li, J.; Zhou, H.-C. Recent Advances in Gas Storage and Separation Using Metal−Organic Frameworks. *Mater. Today* **2018**, *21*, 108−121.

(4) Pascanu, V.; González Miera, G.; Inge, A. K.; Martín-Matute, B. Metal−Organic Frameworks as Catalysts for Organic Synthesis: A Critical Perspective. *J. Am. Chem. Soc.* **2019**, *141*, 7223−7234.

(5) Solanki, V. A.; Borah, B. Ranking of Metal−Organic Frameworks (MOFs) for Separation of Hexane Isomers by Selective Adsorption. *Ind. Eng. Chem. Res.* **2019**, *58*, 20047−20065.

(6) Yang, D.; Gates, B. C. Catalysis by Metal Organic Frameworks: Perspective and Suggestions for Future Research. *ACS Catal.* **2019**, *9*, 1779−1798.

(7) Yaghi, O. M.; O'Keeffe, M.; Ockwig, N. W.; Chae, H. K.; Eddaoudi, M.; Kim, J. Reticular Synthesis and the Design of New Materials. *Nature* **2003**, *423*, 705−714.

(8) Tranchemontagne, D. J.; Mendoza-Cortés, J. L.; O'Keeffe, M.; Yaghi, O. M. Secondary Building Units, Nets and Bonding in the

Chemistry of Metal−Organic Frameworks. *Chem. Soc. Rev.* **2009**, *38*, 1257−1283.
(9) Long, J. R.; Yaghi, O. M. The Pervasive Chemistry of Metal−Organic Frameworks. *Chem. Soc. Rev.* **2009**, *38*, 1213−1214.
(10) O'Keeffe, M.; Yaghi, O. M. Deconstructing the Crystal Structures of Metal−Organic Frameworks and Related Materials into Their Underlying Nets. *Chem. Rev.* **2012**, *112*, 675−702.
(11) Deng, H.; Grunder, S.; Cordova, K. E.; Valente, C.; Furukawa, H.; Hmadeh, M.; Gándara, F.; Whalley, A. C.; Liu, Z.; Asahina, S.; Kazumori, H.; O'Keeffe, M.; Terasaki, O.; Stoddart, J. F.; Yaghi, O. M. Large-Pore Apertures in a Series of Metal-Organic Frameworks. *Science* **2012**, *336*, 1018−1023.
(12) Chatt, J. The Stabilisation of Low Valent States of the Tansition Metals: Introductory Lecture. *J. Inorg. Nucl. Chem.* **1958**, *8*, 515−531.
(13) Ellis, J. E. Adventures with Substances Containing Metals in Negative Oxidation States. *Inorg. Chem.* **2006**, *45*, 3167−3186.
(14) Masoomi, M. Y.; Morsali, A.; Dhakshinamoorthy, A.; Garcia, H. Mixed-Metal MOFs: Unique Opportunities in Metal−Organic Framework (MOF) Functionality and Design. *Angew. Chem., Int. Ed.* **2019**, *58* (43), 15188−15205.
(15) Abednatanzi, S.; Gohari Derakhshandeh, P.; Depauw, H.; Coudert, F.-X.; Vrielinck, H.; Van Der Voort, P.; Leus, K. Mixed-Metal Metal−Organic Frameworks. *Chem. Soc. Rev.* **2019**, *48*, 2535−2565.
(16) Wang, Z.; Cohen, S. M. Postsynthetic modification of metal−organic frameworks. *Chem. Soc. Rev.* **2009**, *38*, 1315−1329.
(17) Cohen, S. M. Postsynthetic Methods for the Functionalization of Metal−Organic Frameworks. *Chem. Rev.* **2012**, *112*, 970−1000.
(18) Li, Z.; Schweitzer, N. M.; League, A. B.; Bernales, V.; Peters, A. W.; Getsoian, A. B.; Wang, T. C.; Miller, J. T.; Vjunov, A.; Fulton, J. L.; Lercher, J. A.; Cramer, C. J.; Gagliardi, L.; Hupp, J. T.; Farha, O. K. Sintering-Resistant Single-Site Nickel Catalyst Supported by Metal−Organic Framework. *J. Am. Chem. Soc.* **2016**, *138*, 1977−1982.
(19) Abdel-Mageed, A. M.; Rungtaweevoranit, B.; Parlinska-Wojtan, M.; Pei, X.; Yaghi, O. M.; Behm, R. J. Highly Active and Stable Single-Atom Cu Catalysts Supported by a Metal−Organic Framework. *J. Am. Chem. Soc.* **2019**, *141*, 5201−5210.
(20) Van Velthoven, N.; Waitschat, S.; Chavan, S. M.; Liu, P.; Smolders, S.; Vercammen, J.; Bueken, B.; Bals, S.; Lillerud, K. P.; Stock, N.; De Vos, D. E. Single-site metal−organic framework catalysts for the oxidative coupling of arenes via C−H/C−H activation. *Chem. Sci.* **2019**, *10*, 3616−3622.
(21) Syed, Z. H.; Sha, F.; Zhang, X.; Kaphan, D. M.; Delferro, M.; Farha, O. K. Metal−Organic Framework Nodes as a Supporting Platform for Tailoring the Activity of Metal Catalysts. *ACS Catal.* **2020**, *10*, 11556−11566.
(22) Goldberg, I. Crystal Engineering of Porphyrin Framework Solids. *Chem. Commun.* **2005**, 1243−1254.
(23) Garibay, S. J.; Stork, J. R.; Cohen, S. M. The Use of Metalloligands in Metal-Organic Frameworks. *Prog. Inorg. Chem.* **2009**, *56*, 335−378.
(24) Kumar, G.; Gupta, R. Molecularly Designed Architectures − the Metalloligand Way. *Chem. Soc. Rev.* **2013**, *42*, 9403−9453.
(25) Burgess, S. A.; Kassie, A.; Baranowski, S. A.; Fritzsching, K. J.; Schmidt-Rohr, K.; Brown, C. M.; Wade, C. R. Improved Catalytic Activity and Stability of a Palladium Pincer Complex by Incorporation into a Metal−Organic Framework. *J. Am. Chem. Soc.* **2016**, *138*, 1780−1783.
(26) Agnew, D. W.; Gembicky, M.; Moore, C. E.; Rheingold, A. L.; Figueroa, J. S. Robust, Transformable, and Crystalline Single-Node Organometallic Networks Constructed from Ditopic *m*-Terphenyl Isocyanides. *J. Am. Chem. Soc.* **2016**, *138*, 15138−15141.
(27) Agnew, D. W.; DiMucci, I. M.; Arroyave, A.; Gembicky, M.; Moore, C. E.; MacMillan, S. N.; Rheingold, A. L.; Lancaster, K. M.; Figueroa, J. S. Crystalline Coordination Networks of Zero-Valent Metal Centers: Formation of a 3-Dimensional Ni(0) Framework with m-Terphenyl Diisocyanides. *J. Am. Chem. Soc.* **2017**, *139*, 17257−17260.
(28) Arroyave, A.; Gembicky, M.; Rheingold, A. L.; Figueroa, J. S. Aqueous Stability and Ligand Substitution of a Layered Cu(I)/Isocyanide-Based Organometallic Network Material with a Well-Defined Channel Structure. *Inorg. Chem.* **2020**, *59*, 11868−11878.
(29) Cotton, F. A.; Zingales, F. The Donor-Acceptor Properties of Isonitriles as Estimated by Infrared Study. *J. Am. Chem. Soc.* **1961**, *83*, 351−355.
(30) Carpenter, A. E.; Mokhtarzadeh, C. C.; Ripatti, D. S.; Havrylyuk, I.; Kamezawa, R.; Moore, C. E.; Rheingold, A. L.; Figueroa, J. S. Comparative Measure of the Electronic Influence of Highly Substituted Aryl Isocyanides. *Inorg. Chem.* **2015**, *54*, 2936−2944.
(31) Malatesta, L.; Bonati, F. *Isocyanide Complexes of Transition Metals*; Wiley: New York, 1969.
(32) Malatesta, L. Palladium(0) Compounds. Part I. Diisonitrilo-palladium(0) Compounds. *J. Chem. Soc.* **1955**, 3924−3926.
(33) Yamamoto, Y. Zerovalent Transition Metal Complexes of Organic Isocyanides. *Coord. Chem. Rev.* **1980**, *32*, 193−233.
(34) Yamamoto, Y.; Yamazaki, H. Low-Valent Isocyanide Complexes and Clusters of Palladium and Platinum. Crystal Structure of $[Pt\{C(=NR)N(R)C(=NR\}(RNC)_2]$(R = 2,6-$Me_2C_6H_3$). *J. Chem. Soc., Dalton Trans.* **1989**, 2161−2166.
(35) Weber, L. Homoleptic Isocyanide Metalates. *Angew. Chem., Int. Ed.* **1998**, *37*, 1515−1517.
(36) Ivasenko, O.; Perepichka, D. F. Mastering Fundamentals of Supramolecular Sesign with Carboxylic Acids. Common Lessons from X-ray Crystallography and Scanning Tunneling Microscopy. *Chem. Soc. Rev.* **2011**, *40*, 191−206.
(37) Adachi, T.; Ward, M. D. Versatile and Resilient Hydrogen-Bonded Host Frameworks. *Acc. Chem. Res.* **2016**, *49*, 2669−2679.
(38) Luo, J.; Wang, J.-W.; Zhang, J.-H.; Lai, S.; Zhong, D.-C. Hydrogen-Bonded Organic Frameworks: Design, Structures and Potential Applications. *CrystEngComm* **2018**, *20*, 5884−5898.
(39) Lin, R.-B.; He, Y.; Li, P.; Wang, H.; Zhou, W.; Chen, B. Multifunctional Porous Hydrogen-Bonded Organic Framework Materials. *Chem. Soc. Rev.* **2019**, *48*, 1362−1389.
(40) Hisaki, I.; Xin, C.; Takahashi, K.; Nakamura, T. Designing Hydrogen-Bonded Organic Frameworks (HOFs) with Permanent Porosity. *Angew. Chem., Int. Ed.* **2019**, *58*, 11160−11170.
(41) Li, P.; Ryder, M. R.; Stoddart, J. F. Hydrogen-Bonded Organic Frameworks: A Rising Class of Porous Molecular Materials. *Acc. Mater. Res.* **2020**, *1*, 77−87.
(42) Fox, B. J.; Sun, Q. Y.; Dipasquale, A. G.; Fox, A. R.; Rheingold, A. L.; Figueroa, J. S. Solution Behavior and Structural Properties of Cu(I) Complexes Featuring *m*-terphenyl Isocyanides. *Inorg. Chem.* **2008**, *47*, 9010−9020.
(43) Fox, B. J.; Millard, M. D.; DiPasquale, A. G.; Rheingold, A. L.; Figueroa, J. S. Thallium(I) as a Coordination Site Protection Agent: Preparation of an Isolable Zero-Valent Nickel Tris-Isocyanide. *Angew. Chem., Int. Ed.* **2009**, *48*, 3473−3477.
(44) Margulieux, G. W.; Weidemann, N.; Lacy, D. C.; Moore, C. E.; Rheingold, A. L.; Figueroa, J. S. Isocyano analogues of $[Co(CO)_4]^n$: A Tetraisocyanide of Cobalt Isolated in Three States of Charge. *J. Am. Chem. Soc.* **2010**, *132*, 5033−5035.
(45) Stewart, M. A.; Moore, C. E.; Ditri, T. B.; Labios, L. A.; Rheingold, A. L.; Figueroa, J. S. Electrophilic functionalization of well-behaved manganese monoanions supported by m-terphenyl isocyanides. *Chem. Commun.* **2011**, *47*, 406−408.
(46) Carpenter, A. E.; Margulieux, G. W.; Millard, M. D.; Moore, C. E.; Weidemann, N.; Rheingold, A. L.; Figueroa, J. S. Zwitterionic Stabilization of a Reactive Cobalt Tris-Isocyanide Monoanion by Cation Coordination. *Angew. Chem., Int. Ed.* **2012**, *51*, 9412−9416.
(47) Carpenter, A. E.; McNeece, A. J.; Barnett, B. R.; Estrada, A. L.; Mokhtarzadeh, C. C.; Moore, C. E.; Rheingold, A. L.; Perrin, C. L.; Figueroa, J. S. Direct Observation of β-Chloride Elimination from an Isolable β-Chloroalkyl Complex of Square-Planar Nickel. *J. Am. Chem. Soc.* **2014**, *136*, 15481−15484.
(48) Mokhtarzadeh, C. C.; Margulieux, G. W.; Carpenter, A. E.; Weidemann, N.; Moore, C. E.; Rheingold, A. L.; Figueroa, J. S.

https://doi.org/10.1021/acs.inorgchem.1c01804
Inorg. Chem. 2021, 60, 12545−12554

Synthesis and Protonation of an Encumbered Iron Tetraisocyanide Dianion. *Inorg. Chem.* **2015**, *54*, 5579−5587.
(49) Carpenter, A. E.; Chan, C.; Rheingold, A. L.; Figueroa, J. S. A Well-Defined Isocyano Analogue of $HCo(CO)_4$. 2: Relative Brønsted Acidity as a Function of Isocyanide Ligation. *Organometallics* **2016**, *35*, 2319−2326.
(50) Carpenter, A. E.; Rheingold, A. L.; Figueroa, J. S. A Well-Defined Isocyano Analogue of $HCo(CO)_4$. 1: Synthesis, Decomposition, and Catalytic 1,1-Hydrogenation of Isocyanides. *Organometallics* **2016**, *35*, 2309−2318.
(51) Mokhtarzadeh, C. C.; Moore, C. E.; Rheingold, A. L.; Figueroa, J. S. Terminal Iron Carbyne Complexes Derived from Arrested CO_2 Reductive Disproportionation. *Angew. Chem., Int. Ed.* **2017**, *56*, 10894−10899.
(52) Chan, C.; Carpenter, A. E.; Gembicky, M.; Moore, C. E.; Rheingold, A. L.; Figueroa, J. S. Associative Ligand Exchange and Substrate Activation Reactions by a Zero-Valent Cobalt Tetraisocyanide Complex. *Organometallics* **2019**, *38*, 1436−1444.
(53) Irving, H.; Jonason, M. (Methyl isocyanide)copper(I) Iodide. *J. Chem. Soc.* **1960**, 2095−2097.
(54) Fisher, P. J.; Taylor, N. E.; Harding, M. M. The Crystal Structure of Cuprous Iodide−Methyl Isocyanide. *J. Chem. Soc.* **1960**, *0*, 2303−2309.
(55) Otsuka, S.; Mori, K.; Yamagami, K. Coordination Effects in Organic Reactions. I. A Novel Preparation of *t*-Alkyl Isocyanide Complexes by *N*-Alkylation of Hydrogen Cyanide. *J. Org. Chem.* **1966**, *31*, 4170−4174.
(56) Benouazzane, M.; Coco, S.; Espinet, P.; Barberá, J. Supramolecular Organization in Copper(I) Isocyanide Complexes: Copper-(I) Liquid Crystals from a Simple Molecular Structure. *J. Mater. Chem.* **2001**, *11*, 1740−1744.
(57) Benouazzane, M.; Coco, S.; Espinet, P.; Barberá, J. Binuclear Mesogenic Copper(I) Isocyanide Complexes with an Unusual Inorganic Core Formed by Two Tetrahedra Sharing an Edge. *Inorg. Chem.* **2002**, *41*, 5754−5759.
(58) Ditri, T. B.; Fox, B. J.; Moore, C. E.; Rheingold, A. L.; Figueroa, J. S. Effective Control of Ligation and Geometric Isomerism: Direct Comparison of Steric Properties Associated with Bis-mesityl and Bis-diisopropylphenyl m-Terphenyl Isocyanides. *Inorg. Chem.* **2009**, *48*, 8362−8375.
(59) Grodzicki, A.; Łakomska, I.; Piszczek, P.; Szymańska, I.; Szłyk, E. Copper(I), silver(I) and gold(I) Carboxylate Complexes as Precursors in Chemical Vapour Deposition of Thin Metallic Films. *Coord. Chem. Rev.* **2005**, *249*, 2232−2258.
(60) Sevryugina, Y.; Rogachev, A. Y.; Petrukhina, M. A. The First Hexanuclear Copper(I) Carboxylate: X-ray Crystal Structure and Reactivity in Solution and Gas-Phase Reactions. *Inorg. Chem.* **2007**, *46*, 7870−7879.
(61) Sevryugina, Y.; Hietsoi, O.; Petrukhina, M. A. Tetranuclear Copper(I) Clusters: Impact of Bridging Carboxylate Ligands on Solid State Structure and Photoluminescence. *Chem. Commun.* **2007**, 3853−3855.
(62) Liu, J.; Xiao, R.; Wong, Y.-L.; Zhou, X.-P.; Zeller, M.; Hunter, A. D.; Fang, Q.; Liao, L.; Xu, Z. Made in Water: A Stable Microporous Cu(I)-carboxylate Framework (CityU-7) for CO_2, Water, and Iodine Uptake. *Inorg. Chem.* **2018**, *57*, 4807−4811.
(63) Etter, M. C. Encoding and Decoding Hydrogen-Bond Patterns of Organic Compounds. *Acc. Chem. Res.* **1990**, *23*, 120−126.
(64) Bosch, M.; Zhang, M.; Zhou, H.-C. Increasing the Stability of Metal-Organic Frameworks. *Adv. Chem.* **2014**, *2014*, 1.
(65) Yuan, S.; Feng, L.; Wang, K.; Pang, J.; Bosch, M.; Lollar, C.; Sun, Y.; Qin, J.; Yang, X.; Zhang, P.; Wang, Q.; Zou, L.; Zhang, Y.; Zhang, L.; Fang, Y.; Li, J.; Zhou, H.-C. Stable Metal−Organic Frameworks: Design, Synthesis, and Applications. *Adv. Mater.* **2018**, *30*, 1704303.
(66) Pangborn, A. B.; Giardello, M. A.; Grubbs, R. H.; Rosen, R. K.; Timmers, F. J. Safe and Convenient Procedure for Solvent Purification. *Organometallics* **1996**, *15*, 1518−1520.
(67) Arnarego, W. L. F.; Chai, C. L. L. *Purification of Laboratory Chemicals*, 5th ed.; Elsevier, 2003.
(68) Fulmer, G. R.; Miller, A. J. M.; Sherden, N. H.; Gottlieb, H. E.; Nudelman, A.; Stoltz, B. M.; Bercaw, J. E.; Goldberg, K. I. NMR Chemical Shifts of Trace Impurities: Common Laboratory Solvents, Organics, and Gases in Deuterated Solvents Relevant to the Organometallic Chemist. *Organometallics* **2010**, *29*, 2176−2179.
(69) Sheldrick, G. A short history of SHELX. *Acta Crystallogr., Sect. A: Found. Crystallogr.* **2008**, *64*, 112−122.
(70) Sheldrick, G. Crystal structure refinement with SHELXL. *Acta Crystallogr., Sect. C: Struct. Chem.* **2015**, *71*, 3−8.
(71) Dolomanov, O. V.; Bourhis, L. J.; Gildea, R. J.; Howard, J. A. K.; Puschmann, H. OLEX2: a complete structure solution, refinement and analysis program. *J. Appl. Crystallogr.* **2009**, *42*, 339−341.

https://doi.org/10.1021/acs.inorgchem.1c01804
Inorg. Chem. 2021, 60, 12545−12554